Temporal Coherence of MgO Based Magnetic Tunnel Junction Spin Torque Oscillators

D. Houssameddine, U. Ebels, and B. Dieny
SPINTEC, CEA, CNRS, UJF, INPG, CEA/INAC, 17 Rue des Martyrs, 38054 Grenoble, France

K. Garello, J.-P. Michel, B. Delaet, B. Viala, and M.-C. Cyrille
CEA, LETI, MINATEC 38054 Grenoble, France

J. A. Katine and D. Mauri
Hitachi Global Storage Technologies, 3403 Yerba Buena Road, San Jose, California 95135, USA
(Received 12 February 2009; published 22 June 2009)

Single-shot, time-resolved measurements are presented to investigate the temporal coherence of the microwave emission for MgO based magnetic tunnel junction spin torque oscillators. The time-domain data reveal that the steady state regime obtained from frequency-domain analysis can be subdivided into two regimes as a function of spin polarized current amplitude. According to these two regimes, two mechanisms that limit the temporal coherence are identified. At low current, extinctions of the steady state oscillations lead to a very short coherence time on the order of a few nanoseconds, while at higher current, the extinctions vanish and the coherence time saturates around 40 ns. As an important result it is shown that the latter is limited by frequency fluctuations. Quenching these frequency fluctuations suggests an intrinsic linewidth that is by a factor of 20 below the one of the free running oscillator.

DOI: 10.1103/PhysRevLett.102.257202 PACS numbers: 85.75.−d, 72.25.−b, 75.75.+a

The spin transfer effect has been shown to be a powerful alternative to external magnetic fields in manipulating the magnetization state of a thin magnetic nanoelement [1,2]. One important manifestation of this effect is the ability to generate periodic large amplitude magnetization oscillations [3,4] and to investigate the associated nonlinear dynamic properties. Previous experiments have been performed to reveal the nature of these oscillations as a function of current [3], applied field amplitude [3], applied field orientation [5] and magnetization configuration [6–8]; one of the major fundamental issues that remains to be addressed for spin transfer torque oscillators (STOs) is the linewidth.

In the frame of general oscillator theories, the linewidth of a free running oscillator is composed of two contributions: (i) an ''intrinsic'' linewidth due to phase noise and (ii) frequency fluctuations, which result in a broadening of the linewidth envelope. Distinguishing these two contributions is possible when the time scales of the phase fluctuations and the frequency fluctuations are different. Recently it has been shown that STOs can be described in terms of such general oscillator models when using nonlinear spin wave theory [9,10]. Within this theory it was shown that the intrinsic phase noise is renormalized by frequency fluctuations via the nonlinear dependence of the frequency on the oscillation amplitude. In a real STO device however, other contributions to the frequency fluctuations might exist. Using single-shot time-resolved measurements [8,11], we show that frequency fluctuations exist for STOs, and provide an estimate of the time scale of these fluctuations.

The STO devices studied here are MgO based magnetic tunnel junctions (MTJ) whose spin transfer driven microwave emission peaks are characterized by large output power and narrow linewidth. Details of the samples and their general microwave properties can be found in our previous work [12]. Here, we focus on a 40% TMR device (called LTMR device in Ref. [12]) with circular shape of 90 nm diameter. All data presented have been taken on a single device but results are general for this given geometry. A typical microwave emission spectrum of the free layer in the antiparallel (AP) configuration is presented in Fig. 1(a) as measured with a spectrum analyzer.

The corresponding dependence of the oscillation frequency on the current is given in Fig. 1(b), where according to Ref. [12], TFMR corresponds to thermally activated ferromagnetic resonance excitations and STT denotes the spin-torque induced steady state regime of excitations. Based on the Kim-Slavin-Tiberkevich model [9,10], the transition between the thermally activated ferromag-

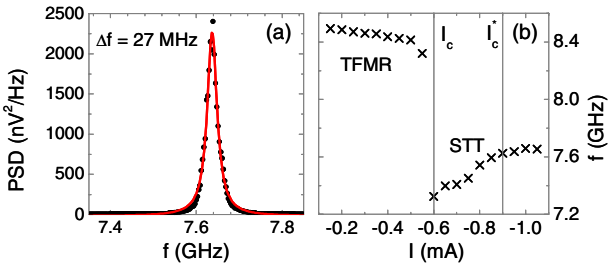

FIG. 1 (color online). (a) Free layer microwave emission peak (1st harmonics) for an external field of 57.5 mT (AP state) and a bias current of −0.95 mA. (b) Current dependence of the emission frequency. A clear jump is observed at $I_c = -0.60$ mA. I_c^* is defined in the text.

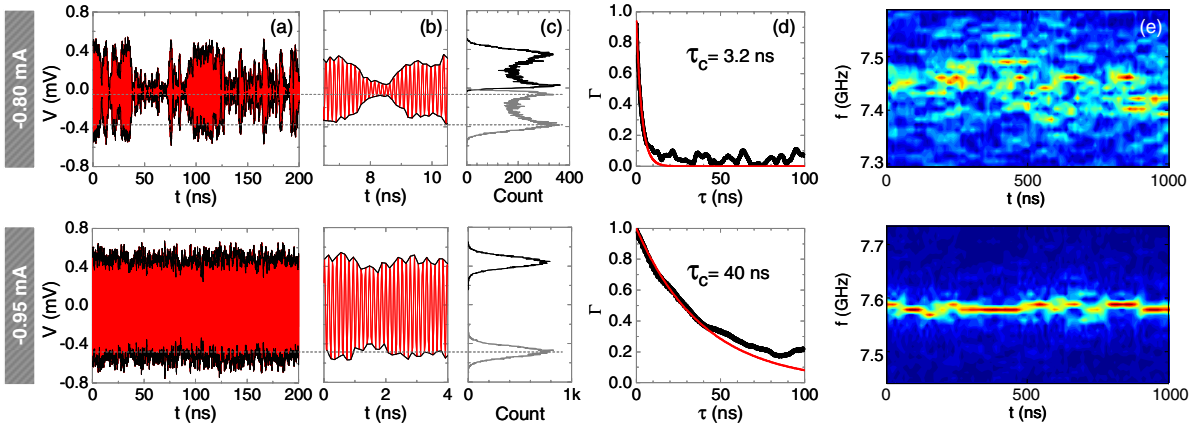

FIG. 2 (color online). Time trace analysis for applied currents of −0.80 mA (top) and −0.95 mA (bottom). (a) 200 ns segment of the full time trace (gain corrected). The signal is shown in red and the positive and negative envelopes in black. (b) 4 ns zoom revealing the high frequency oscillations. (c) Histogram of the positive (black) and negative (grey) signal envelopes. (d) Envelope of the autocorrelation $\Gamma(\tau)$ deduced from the full time trace (black) and exponentially decaying fit (red). (e) Time-frequency spectrogram extracted from a gliding window FFT analysis (see text).

netic resonance regime and the STT sustained regime is blurred by thermal activation. The critical current is inferred from frequency-domain studies by a minimum of the linewidth vs current which is accompanied by a strong increase in the emitted power (precession amplitude) and a fairly clear shift of the oscillation frequency. While these criteria are not strictly valid for the devices studied here, we still obtain a rather abrupt increase of the integrated power of the microwave emission peak which is accompanied by an abrupt downward jump of the frequency. For the sample of Fig. 1(b) the jump suggests that the critical current of the steady state regime is $I_c = -0.60$ mA. In the following, we show from time-domain studies that the distinction between these two regimes has to be redefined.

The time-domain experimental setup used here is similar to those used in the frequency domain where the spectrum analyzer is replaced by a high speed real time oscilloscope of 12 GHz bandwidth and 40 Gsamples/s sampling rate. The signal is first amplified by a 27 dB amplifier and then passed through a cavity filter characterized by a −1 dB band of 7 to 8 GHz and 20 dB/GHz slopes. This filter is flat over the full range of STO frequencies in the current range $|I| > |I_c|$. The filter assures, for the STO emission peaks of interest, proper extraction of the relevant parameters from the time domain signal traces upon rejecting low frequency noise, harmonics related contributions and background noise. In particular the background noise level of the amplified signal is reduced from 1.5 to 0.7 mV.

For the sample of Fig. 1 time traces of 100 μs have been acquired in the current range of −0.60 to −1.10 mA. A 200 ns long segment of the total time trace is presented in Fig. 2(a) for $I = -0.80$ and −0.95 mA, and a 4 ns zoom is given in Fig. 2(b) while the corresponding amplitude envelope histograms are shown in Fig. 2(c). For $I = -0.80$ mA, two contributions to the signal are observed: a high amplitude signal that lasts up to a few tens of nanoseconds at most and a low amplitude noise, that we call extinction. These extinctions mean that for a bias current of −0.80 mA, the STO oscillation is only partially sustained over a short time scale, and that it vanishes from time to time (most likely due to thermal activation), giving rise to an overall telegraph-noise-like signal. The relative occurrence of the extinctions can be quantified by the envelope histogram of Fig. 2(c). Here, for −0.80 mA, the histogram count of the low amplitude peak due to extinctions is equal to the count of the high amplitude signal peak voltage, meaning that extinctions are very frequent. In contrast, for an applied current of −0.95 mA, only the high amplitude signal peak exists, meaning that the oscillations are sustained over long (μs) time scales without extinctions. From the vanishing of the low amplitude peak (extinctions) in the envelope histogram we can define a critical current I_c^* for which a true stationary steady state is reached over long time scales. The corresponding value $I_c^* = -0.90$ mA is different from the critical current $I_c = -0.60$ mA deduced from frequency-domain experiments, Fig. 1(b). The time-domain measurements thus clearly show that the steady state regime can be subdivided into two regions: one of an intermittent steady state (short term) and one of a true stationary steady state (long term).

In the following, we quantify the temporal coherence of the STO signal for these two regions and compare it to the linewidth obtained in the frequency-domain. Quite generally, in the frequency-domain the linewidth is obtained from a Lorentzian fit of the power spectral density (PSD), such as shown in Fig. 1(a). By definition the PSD is equal to the Fourier transform (FT) of the autocorrelation function $\Gamma(\tau)$ of the real signal $s(t)$:

$$\Gamma(\tau) = \int_{-\infty}^{+\infty} s(t)s(t-\tau)dt. \quad (1)$$

Furthermore, a Lorentzian line shape of the PSD means

that the autocorrelation function is an exponentially decaying function characterized by a time constant τ_c, that is related to the linewidth via $\Delta f = 1/\pi\tau_c$:

$$\mathrm{PSD} = \mathrm{FT}[\Gamma(\tau)] = \mathrm{FT}[e^{-|t|/\tau_c}] = \frac{2}{\pi}\frac{\Delta f}{\Delta f^2 + 4f^2}. \quad (2)$$

We therefore deduce the autocorrelation function and the corresponding decay time τ_c from the time traces by replacing $\Gamma(\tau)$ by a discrete sum over 625 ns. In Fig. 2(d) the normalized envelope of the autocorrelation function is plotted for $I = -0.80$ and -0.95 mA (black line) which can be fit by an exponentially decaying function (red line) with a characteristic decay time τ_c that defines the temporal coherence of the STO signal. In Fig. 3(a) τ_c is summarized as a function of the current amplitude. In Fig. 3(b), we compare the inverse of the coherence time (red dots) with the linewidth Δf deduced from the Lorentzian fit to the peaks measured by a spectrum analyzer (black crosses). The good agreement between these two parameters shows that the coherence time acquired on a μs time scale is representative for the coherence of the PSD acquired in the frequency-domain over much longer time scales. It furthermore means that no other processes have to be considered that limit the temporal coherence in the frequency-domain studies.

With this, we can now analyze in more detail the temporal coherence time τ_c of Fig. 3(a) distinguishing two regimes. For $|I| < |I_c^*|$, τ_c is small and reveals an exponential increase upon increasing current amplitude [dots and red line in Fig. 3(a)]. For $|I| > |I_c^*|$, τ_c saturates around a value of 40 ns. These two regimes reflect the fact that different processes limit the temporal coherence. For $|I| < |I_c^*|$ we see from a statistical analysis that the average time interval over which a signal "burst" exists between two extinctions is equal to the coherence time τ_c and conclude that here the dominant processes limiting the temporal coherence are signal extinctions. For $|I| > |I_c^*|$ the extinctions vanish and the coherence time should reach very large values as suggested by the exponential growth of the fit in Fig. 3(a) (solid line). The fact that τ_c saturates around 40 ns (which is much smaller than the length of a signal) means that another process starts to dominate the temporal coherence. We show in the following that in this case τ_c is limited by frequency fluctuations. For this, we performed a gliding window FFT over 100 ns long segments of the full traces by gliding the selected time window in steps of 1 ns. The corresponding FFT spectra vs time are quite different for $I = -0.80$ and -0.95 mA; see Fig. 2(e). For -0.80 mA, a 100 ns segment is composed of several signal bursts and the corresponding FFT therefore shows several frequency components simultaneously. This means essentially that every time the oscillator is "turned on" the frequency is slightly different. For $I = -0.95$ mA, the time trace corresponds to a stationary oscillation and there is only one frequency component in a 100 ns time window.

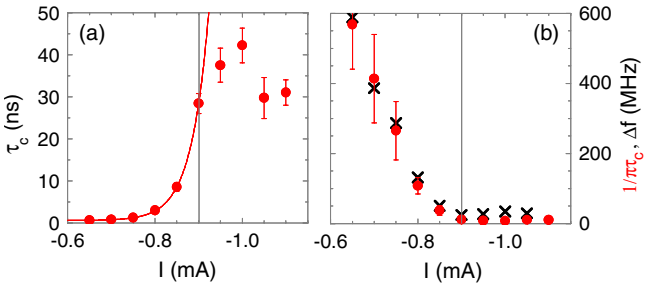

FIG. 3 (color online). (a) Coherence time τ_c (dots) vs current exponential fit (solid line). (b) Red dots: the inverse of the coherence time $1/\pi\tau_c$. Black cross: spectral linewidth extracted from Lorentzian fits of spectrum analyzer measurements.

As we can see from Fig. 2(e), this frequency fluctuates in time. Note that the apparent discrete jumps in frequency are an artifact due the limited frequency resolution which is discretized into 10 MHz "channels" due to the finite length (100 ns) of the segment used for the FFT. These jumps should therefore not be confused with discrete oscillator modes. For higher resolution we expect the frequency to fluctuate continuously from one frequency channel to the next. A statistical analysis of Fig. 2(e) reveals that the average time over which the frequency is stable within 10 MHz is about 80 ns. This is larger but on the order of the decay time τ_c deduced from the autocorrelation function; see Fig. 2(d) for $I = -0.95$ mA. We can therefore conclude that the temporal coherence in the steady state regime $|I| > |I_c^*|$ is limited by frequency fluctuations. This is a much slower fluctuation rate than the signal extinctions at lower current and consequently the process of frequency fluctuations becomes dominant only when the extinctions vanish or when the average length of the signal burst is much larger than 40 ns.

Taking frequency fluctuations into account, we can now, in the regime $|I| > |I_c^*|$, interpret the free running oscillator signal measured by the spectrum analyzer as the envelope of a narrow peak whose frequency fluctuates in time. The next point is then to estimate the intrinsic linewidth of this narrow fluctuating peak. For this let us first note that the linewidth of 24 MHz obtained from the FFT of a 1.6 μs time trace, Fig. 4(a), corresponds to the one measured by a spectrum analyzer (27 MHz), Fig. 1(a) ($I = -0.95$ mA). In order to determine the intrinsic linewidth of the narrow fluctuating peak with sufficient resolution, one has to analyze a long enough signal trace for which the frequency fluctuations are quenched. We therefore isolated and concatenated time trace segments with a central frequency of 7.58 GHz $\pm$ 5 MHz with no other secondary peak in the spectrum. From this, we built a 740 ns long time trace yielding a frequency resolution of 1.4 MHz. The PSD obtained from the corresponding FFT shows a very sharp main peak; see Fig. 4(b). Although it is not possible to use a Lorentzian fit due to the resolution limit; Fig. 4(b) shows that the intrinsic linewidth lies in the sub-MHz range. This is thus an upper estimation for the linewidth

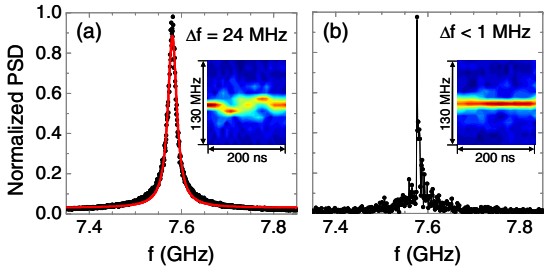

FIG. 4 (color online). (a) Dots: long time scale emission peak for −0.95 mA obtained from an average of 60 FFTs performed on 1.6 μs continuous time traces, including frequency fluctuations as suggested by the inset. The peak has a Lorentz line shape with a linewidth of 24 MHz. (b) FFT performed on concatenated time traces with ''fixed'' frequency as suggested by the inset. The resolution is 1.4 MHz.

of the narrow fluctuating peak, which is a factor of 20 smaller than the free running spectrum analyzer linewidth.

With this analysis, the remaining question to address will be on the physical origin of the intrinsic linewidth and of the frequency fluctuations. From the theoretical models mentioned in the introduction [9,10], one might be tempted to identify the intrinsic linewidth with phase noise (due to stochastic noise) and the frequency fluctuations with the nonlinear renormalization of this phase noise due to the nonlinear frequency-amplitude dependence. In this hypothesis, frequency fluctuations should be directly related to voltage amplitude noise. For this several noise contributions have to be considered, both extrinsic (measurement related) and intrinsic (STO device related). Extrinsic sources are biasing field and current fluctuations due to instabilities of the sources, the white background noise of the measurement chain and an artificial sampling noise due to limited sampling rate. Source fluctuations can be neglected on the studied time scale due to their limited bandwidth (kHz). The white background noise can be evaluated from the voltage amplitude histogram [such as in Fig. 2(c)] at zero bias current. It is then removed by considering that the total noise is a convolution of the white background noise and the STO noise. The sampling rate noise has been taken into account through simulations of discrete sinusoidal signal with random Gaussian noise. After removing the extrinsic noise contributions, we compared the intrinsic amplitude noise level of the total time trace (100 μs) containing the frequency fluctuations and of the time trace for the concatenated signal and found exactly the same value. From this we conclude that if fluctuations of the precession amplitude were the dominant contribution to the frequency fluctuations one would expect that the ''fixed'' frequency signal trace has a reduced amplitude noise level which is not the case. Therefore for the devices studied here it seems that amplitude noise is not the main contribution to the frequency fluctuations. This is consistent with the fact that in the range of $|I| > |I_c^*|$ the slope of df/dI is relatively flat, see Fig. 1(b), indicating a weak nonlinear frequency-amplitude dependence. This leaves as the origin of the frequency fluctuations for instance variations of dipolar coupling fields or fluctuations of the magnetization configuration (mode profile) while voltage amplitude fluctuations might still result from fluctuations of the magnetization trajectory but also from electronic noise of the tunnel junction (resistance and/or tunneling current fluctuations).

To conclude, using single-shot, time-resolved measurements, we have shown that the critical current I_c inferred in the frequency-domain represents only the onset of an intermittent oscillation whose temporal coherence is limited by the occurrence of extinctions ($\tau_c < 10$ ns). The stationary steady state is reached at higher current values $|I_c^*| > |I_c|$. Its temporal coherence is limited by frequency fluctuations with $\tau_c = 40$ ns and is responsible for the frequency-domain linewidth, while the intrinsic linewidth of the fluctuating peak is much narrower. The results shown here underline the importance of time-domain analysis in order to reveal the intrinsic mechanisms responsible for the STO linewidth and temporal coherence. These mechanisms have to be known before addressing experiments on mutual phase locking [13,14] of STOs or on phase noise.

We acknowledge A. Schuhl and P. Vincent for fruitful discussions as well as the referee for his comments on the experimental setup and the discussion on the frequency fluctuations. This work has been supported in part by the French National Agency (ANR) through the Institute CARNOT program as well as by OSEO/ANVAR

[1] J. C. Slonczewski, J. Magn. Magn. Mater. **159**, L1 (1996); **195**, 261 (1999).
[2] L. Berger, Phys. Rev. B **54**, 9353 (1996).
[3] S. I. Kiselev *et al.*, Nature (London) **425**, 380 (2003); W. H. Rippard *et al.*, Phys. Rev. Lett. **92**, 027201 (2004); Q. Mistral *et al.*, Appl. Phys. Lett. **88**, 192507 (2006).
[4] A. V. Nazarov *et al.*, J. Appl. Phys. **103**, 07A503 (2008).
[5] W. H. Rippard *et al.*, Phys. Rev. B **70**, 100406(R) (2004).
[6] M. R. Pufall, W. H. Rippard, M. L. Schneider, and S. E. Russek, Phys. Rev. B **75**, 140404(R) (2007).
[7] V. S. Pribiag *et al.*, Nature Phys. **3**, 498 (2007).
[8] M. R. Pufall, W. H. Rippard, M. L. Schneider, and S. E. Russek, Phys. Rev. B **75**, 140404(R) (2007).
[9] J. V. Kim, V. S. Tiberkevich, and A. N. Slavin, Phys. Rev. Lett. **100**, 017207 (2008).
[10] V. S. Tiberkevich, A. N. Slavin, and J.-V. Kim, Phys. Rev. B **78**, 092401 (2008); Appl. Phys. Lett. **91**, 192506 (2007).
[11] I. N. Krivorotov *et al.*, Science **307**, 228 (2005); I. N. Krivorotov, N. C. Emley, R. A. Buhrman, and D. C. Ralph, Phys. Rev. B **77**, 054440 (2008).
[12] D. Houssameddine *et al.*, Appl. Phys. Lett. **93**, 022505 (2008).
[13] S. Kaka *et al.*, Nature (London) **437**, 389 (2005); F. B. Mancoff, N. D. Rizzo, B. N. Engel, and S. Tehrani, Nature (London) **437**, 393 (2005).
[14] B. Georges *et al.*, Phys. Rev. Lett. **101**, 017201 (2008).